Food Chemistry 340 (2021) 128132

Contents lists available at ScienceDirect

Food Chemistry

journal homepage: www.elsevier.com/locate/foodchem

Short communication

Degree of crosslinking in β-cyclodextrin-based nanosponges and their effect on piperine encapsulation

Juan Guineo-Alvarado[a], Marcela Quilaqueo[b,c], Jeyson Hermosilla[b,c], Sofía González[b,c], Camila Medina[b,c], Aldo Rolleri[d], Loong-Tak Lim[e], Mónica Rubilar[b,c,*]

[a] Master of Engineering Sciences with Specialization in Biotechnology, Universidad de La Frontera, Temuco, Chile
[b] Department of Chemical Engineering, Faculty of Engineering and Science, Universidad de La Frontera, Temuco, Chile
[c] Scientific and Technological Bioresource Nucleus, BIOREN, Universidad de La Frontera, Avenida Francisco Salazar, 01145 Temuco, Chile
[d] Institute of Forests and Society, Faculty of Forest Science and Natural Resources, Universidad Austral de Valdivia, Valdivia, Chile
[e] Department of Food Science, University of Guelph, Guelph, Ontario, N1G2W1, Canada

ARTICLE INFO

Keywords:
Nanosponges
Microwave-assisted fusion
Piperine
β-cyclodextrin

ABSTRACT

Piperine (PIP) is an alkaloid which is potent as a therapeutic agent. However, its applications are restricted by its poor water solubility. Nanosponges (NS) derived from polymers are versatile carriers for poor water-soluble substances. The aim of this work was to synthesize β-cyclodextrin NS, by microwave-assisted fusion, for the encapsulation of PIP. Different formulations of NS were synthesized by varying the molar ratio of β-cyclodextrin:diphenyl carbonate (β-CD:DPC; 1:2, 1:6 and 1:10). NS specimens derived from 1:2, 1:6 and 1:10 β-CD:DPC molar ratios exhibited degree of substitution values of 0.345, 0.629 and 0.878, respectively. The crystallinity of NS was enhanced by increasing diphenyl carbonate concentration. A high degree of crosslinking in the NS increased the loading efficiency due to increased surface area available for bioactive inclusion. This study demonstrated the feasibility of synthesizing NS derived from β-cyclodextrin of high crystallinity for the encapsulation of PIP at high loading capacity.

1. Introduction

Black pepper (*Piper nigrum*) is a plant of the Piperaceae family, largely used as a flavoring agent in foods. Black pepper contains bioactive ingredients in its oleoresin fraction, such as essential oils and piperine (PIP) (Shityakov et al., 2019; Zarai, Boujelbene, Salem, Gargouri & Sayari, 2013). PIP is an alkaloid which possesses diuretic, anti-asthmatic, analgesic, antipyretic, central nervous system depressant, anti-inflammatory, antitumor, and hepatoprotective activities (Shityakov et al., 2019; Swapna, Junise, Shibin, Senthila & Rajesh, 2012). However, the use of PIP in foods and biomedical applications is restricted due to its poor water solubility, low bioavailability, high instability, and spicy-bitter taste (Garrido et al., 2019; Shityakov et al., 2019). Some attempts have been made to develop novel PIP formulations to enhance its solubility and bioavailability using encapsulated PIP (Garrido et al., 2019; Shityakov et al., 2019; Quilaqueo et al., 2019).

Nanosponges (NS) are a novel class of hyper-crosslinked polymers based on colloidal structures consisting of solid nanoparticles with colloidal sizes and nanosized cavities (Tejashri, Amrita & Darshana, 2013). These particles can carry both lipophilic and hydrophilic substances, thereby improving the solubility of poorly water-soluble compounds (Subramanian, Singireddy, Krishnamoorthy & Rajappan, 2012). Cyclodextrins (CD) with suitable crosslinking reagents are materials used to form NS (Shringirishi et al., 2014). CD are cyclic oligomers widely used in the food industry as food additives, for the stabilization of flavors, for taste modifications and the elimination of undesirable tastes and odors and for food preservation (Astray, Gonzalez-Barreiro, Mejuto, Rial-Otero & Simal-Gándara, 2009; Astray, Mejuto, Morales, Rial-Otero & Simal-Gándara, 2010). CD can form inclusion complexes with a wide variety of bioactives to improve their solubility and protect them (Cid, Astray, Morales, Mejuto & Simal-Gandara, 2018; Rakmai, Cheirsilp, Mejuto, Simal-Gándara & Torrado-Agrasar, 2018; Rakmai, Cheirsilp, Mejuto, Torrado-Agrasar & Simal-Gándara, 2017; Rakmai, Cheirsilp, Torrado-Agrasar, Simal-Gándara & Mejuto, 2017). Among the α-, β- and γ-cyclodextrins, NS are generally prepared from β-cyclodextrin (β-CD) because it has the highest complexing ability and stability when treated with crosslinking agents. Low production costs, higher productive rates, and its generally recognized as safe (GRAS) status are some of the advantages of using β-CD for the preparation of

* Corresponding author at: BIOREN, Universidad de La Frontera, Avenida Francisco Salazar, 01145 Temuco, Chile.
E-mail address: monica.rubilar@ufrontera.cl (M. Rubilar).

https://doi.org/10.1016/j.foodchem.2020.128132
Received 8 January 2020; Received in revised form 26 August 2020; Accepted 16 September 2020
Available online 21 September 2020

Table 1
FTIR analyses: absorbance values of peak features and degree of substitution (DS) of nanosponges (NS) synthesized at different synthesis times, β-cyclodextrin (β-CD) and maltodextrin (MD) used as controls.

Samples	$(C=O)^1$ $1748cm^{-1}$	$(O-C=O-O)^2$ $1256cm^{-1}$	$(C-O-C)^3$ $1151cm^{-1}$	CDring $945cm^{-1}$	Cyclic Carbonate $1810cm^{-1}$	DS A_{1748}/A_{1151}
NS 1:2						
7.5 min	0.027	0.033	0.132	0.013	0.003	0.205
15 min	0.029	0.036	0.107	0.013	0.002	0.269
30 min	0.037	0.048	0.107	0.008	0.002	0.345
45 min	0.018	0.021	0.108	0.016	0.001	0.166
NS 1:6						
7.5 min	0.050	0.057	0.123	0.011	0.005	0.407
15 min	0.040	0.049	0.085	0.008	0.002	0.476
30 min	0.036	0.046	0.058	0.004	0.002	0.629
45 min	0.021	0.028	0.071	0.007	0.001	0.299
NS 1:10						
7.5 min	0.048	0.062	0.067	0.007	0.004	0.716
15 min	0.036	0.048	0.041	0.001	0.002	0.878
30 min	0.051	0.063	0.059	0.004	0.005	0.861
45 min	0.045	0.058	0.060	0.008	0.003	0.758
Controls						
β-CD	0.000	0.003	0.098	0.030	0.000	0.000
MD	0.001	0.000	0.044	0.000	0.000	0.000

$(C=O)^1$ Carbonyl group. $(O-C=O-O)^2$ Ester group. $(C-O-C)^3$ Glycosidic bonds. (CD ring) "Breathing" of cyclodextrin ring.

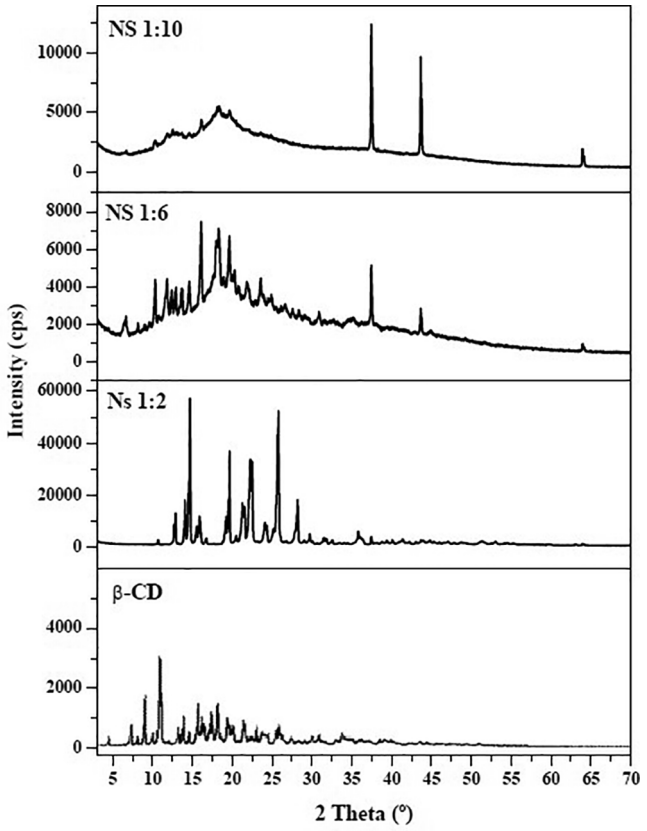

Fig. 1. X-ray diffractograms of β-cyclodextrin (β-CD) and nanosponge (NS) at 1:2, 1:6 and 1:10 β-cyclodextrin:diphenyl carbonate molar ratios.

NS (Tejashri et al., 2013).

The second component involved in the synthesis of NS is the crosslinking agent. The type of crosslinking agent used in the synthesis determines the nature of the nanochannels formed between the cyclodextrin monomers. If NS with hydrophobic nanochannels are required, carbonyldiimidazole, diisocyanates or diphenyl carbonate (DPC) can be used (Tejashri et al., 2013). NS crosslinked with DPC have been synthesized to encapsulate a large number of bioactives (such as camptothecin, quercetin, telmisartan, and gabapentin) with a wide range of applications (Minelli et al., 2012; Singireddy et al., 2016; Singireddy & Subramanian, 2014; Swaminathan et al., 2010; Rao, Bajaj, Khole, Munjapara & Trotta, 2012; Rao & Bhingole, 2015).

Currently, methods of synthesis for NS involved the use of solvent, assisted by ultrasound, conventional heating and microwave-assisted fusion (Osmani et al., 2018; Shringirishi et al., 2014). Microwave-assisted fusion has been successfully used for NS synthesis (Osmani et al., 2018; Singireddy, Pedireddi, Nimmagadda & Subramanian, 2016), which allowed morphological changes and loading of bioactives of interest. Microwave technology has several advantages over conventional heating, such as non-contact heating (reduced surface overheating of the material), radiation instead of conduction heating, selective heating of material, fast start/stop cycle, and the inverse thermal effect (i.e., heating from inside of the material instead of the surface) (Bardts, Gonsior & Ritter, 2008; Bogdal, Penczek, Pielichowski & Prociak, 2003; Hoogenboom & Schubert, 2007; Wiesbrock, Hoogenboom & Schubert, 2004).

Although there are some studies on encapsulation of PIP with β-CD, there is no information on encapsulation using NS with microwave-assisted fusion. In this study, we hypothesized that changes in molar ratios of the polymer and crosslinking agent can alter the degree of crosslinking. High degree of crosslinking can result in higher NS porosity, thereby increasing the PIP loading capacity due to the high interconnection among cyclodextrin monomers. The aim of this work was to synthesize NS using β-cyclodextrin:diphenyl carbonate (β-CD:DPC) with different molar ratios (1:2, 1:6 and 1:10) by microwave-assisted fusion to encapsulate PIP. The synthesis times, physicochemical characteristics of the obtained NS, and the effect of the degree of crosslinking on PIP loading efficiency in the polymer matrix were evaluated.

2. Materials and methods

2.1. Materials

β-CD (purity ≥ 97%, molecular weight 1,134.98 g mol^{-1}), DPC (purity 99%, molecular weight 214.22 g mol^{-1}) and PIP (purity ≥ 97%, molecular weight 285.34 g mol^{-1}) were purchased from Sigma-Aldrich (USA). Ethanol (purity ≥ 99.5%) was purchased from Merck (Germany).

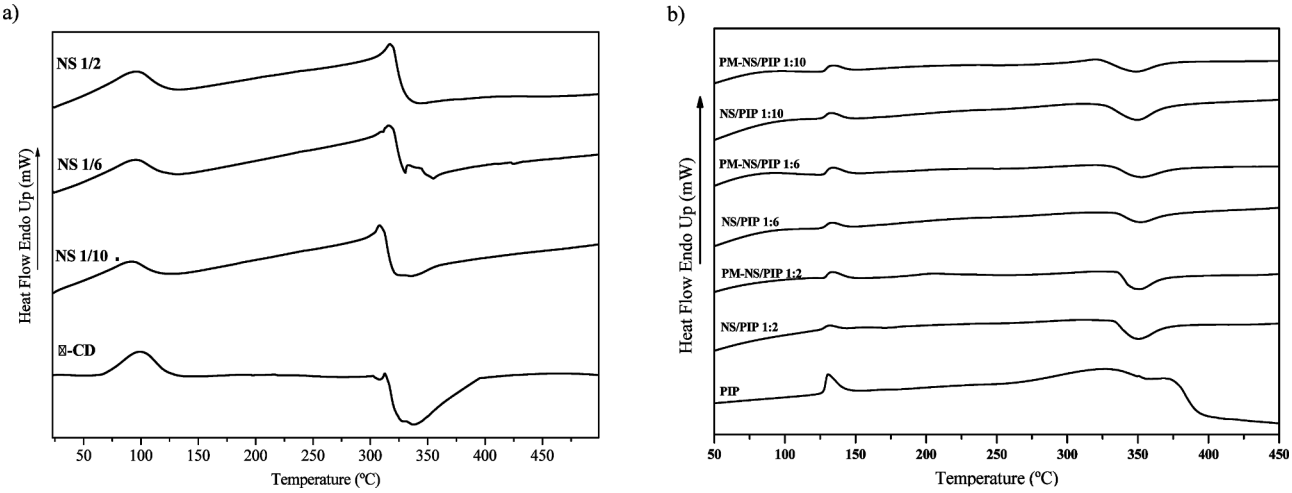

Fig. 2. DSC thermograms of: (a) plain nanosponges (NS) at 1:2, 1:6 and 1:10 β-cyclodextrin:diphenyl carbonate (β-CD:DPC) molar ratios and pure β-CD; (b) plain nanosponge:piperine inclusion complexes (NS:PIP) (NS 1:2, 1:6 and 1:10 β-CD:DPC molar ratios), physical mixture of NS with PIP (PM-NS/PIP) (NS 1:2, 1:6 and 1:10 -CD:DPC molar ratios) and pure PIP.

Table 2
Load efficiencies (LE) of PIP for 1:2, 1:6 and 1:10 β-cyclodextrin:diphenyl carbonate (β-CD:DPC) molar ratios nanosponges (NS) using dichloromethane (DMC), ethanol (ETH) and acetone (ACET) as solvents in the loading process.

NS:PIP ratio	Solvent	β-CD:DPC molar ratios of NS		
		1:2	1:6	1:10
1:2	DMC	78.77 ± 14.25 ^{aB}	55.95 ± 1.17 ^{abB}	72.22 ± 13.96 ^{bB}
	ACET	68.53 ± 14.79 ^{aB}	83.65 ± 8.58 ^{abB}	84.71 ± 4.90 ^{bB}
	ETH	58.24 ± 6.51 ^{aB}	77.61 ± 10.91 ^{abB}	68.69 ± 18.38 ^{bB}
1:1	DMC	50.40 ± 9.51 ^{aA}	56.44 ± 12.15 ^{abA}	66.65 ± 0.59 ^{bA}
	ACET	70.93 ± 4.00 ^{aA}	56.09 ± 22.33 ^{abA}	54.37 ± 4.80 ^{bA}
	ETH	59.17 ± 2.24 ^{aA}	62.94 ± 3.52 ^{abA}	64.34 ± 9.14 ^{bA}
2:1	DMC	74.39 ± 6.40 ^{aB}	84.97 ± 2.87 ^{abB}	76.14 ± 3.65 ^{bB}
	ACET	54.90 ± 3.97 ^{aB}	81.23 ± 7.52 ^{abB}	61.95 ± 18.29 ^{bB}
	ETH	65.48 ± 7.16 ^{aB}	66.74 ± 7.53 ^{abB}	77.76 ± 7.64 ^{bB}

Means of 3 replicates with different superscript letters in columns are significantly different ($p \leq 0.05$) for one-way ANOVA and Duncan's test with NS (small letters), NS:PIP ratio (capital letters). The variable solvent is not significant

2.2. Synthesis of β-cyclodextrin nanosponges

The β-CD-based NS samples were prepared by microwave-assisted synthesis with DPC as the crosslinker, according to Gaidamauskas, Norkus, Butkus, Crans & Grinciene, 2009 and Swaminathan et al. (2010) with some modifications. The molar ratios of β-CD:DPC were 1:2, 1:6 and 1:10. The β-CD:DPC mixture was heated to 180 °C in the microwave synthesizer (CEM Discover SP, North Carolina, USA) with a pre-heating time of 5 min and a reaction time of 30 min, followed by a rapid cooling to 60 °C. The product obtained was subjected to 2 washing cycles with Milli-Q water and 3 cycles of Soxhlet extraction with fresh ethanol in each cycle. The purified product was then dried overnight in an oven at 60 °C and subsequently ground in a mortar. The NS were stored in a desiccator at room temperature until further use.

2.3. Fourier transform infrared (FTIR) spectroscopy

The NS synthesis and PIP inclusion in NS were determined by a Thermo Scientific Nicolet IS5 FTIR spectrometer equipped with ATR ID5 diamond crystal (Thermo Scientific, Germany). Infrared spectra of β-CD, maltodextrin (MD), and PIP were scanned. MD was used here as a control to evaluate the hydrolysis of β-CD during NS synthesis, on the basis that MD shows no absorbance at 945 cm^{-1} due to its linear structure (Garrido et al., 2019). Samples were analyzed in triplicate. The spectra were obtained in the region from 4000 to 650 cm^{-1} using a resolution of 4 cm^{-1}.

In addition, the degree of substitution (DS), which is an index of NS formation, was calculated by Eq. (1), where A_{1748} is the absorbance of carbonyl groups (C═O) at 1748 cm^{-1} and A_{1151} is the absorbance of glycosidic bonds in the NS (Challa, Ahuja, Ali & Khar, 2005; Trotta, Moraglio, Marzona & Maritano, 1993).

$$Degree\ of\ substitution = A_{1749}/A_{1151} \quad (1)$$

2.4. Piperine-loaded nanosponges (NS:PIP).

PIP was suspended in ethanol, acetone or dichloromethane (30 mL) and agitated with magnetic stirring for 15 min. Then, NS was added at different NS:PIP ratios (2:1, 1:1 and 1:2 w/w) and dispersed in a magnetic stirrer. The solvent was evaporated (approximately 24 h) in a fume hood at room temperature. The mixtures were subjected to a gentle washing with ethanol to remove the PIP from NS surfaces. The resulting products were dried at 60 °C for 12 h in an oven to remove residual solvent (Pushpalatha, Selvamuthukumar & Kilimozhi, 2018). The NS:PIP samples were stored in a desiccator at room temperature until later use.

2.5. Loading efficiency (LE)

A weighed amount of 0.01 g NS:PIP was dissolved in 20 mL of ethanol. The sample was then kept at 60 °C in a WiseCircu bath circulator model WCR-P8 (Daihan Scientific., Seoul, Korea) and sonicated

Table 3
FTIR analyses of frequency shift in nanosponge:piperine (NS:PIP) complexes with respect to piperine (PIP) and for 1:2, 1:6 and 1:10 β-cyclodextrin:diphenyl carbonate (β-CD:DPC) molar ratios in loaded nanosponges.

Piperine origin band	Δ shift NS:PIP 1:2			Group	Assignments of PIP vibrations of bonds	Reference
(cm^{-1})	1:2	1:6	1:10			
1633	−2	−2	−2	C═C–C═C	Symmetric stretching of conjugated diene	Pentak, 2016
1610	+1	0	0	C═C–C═C	Asymmetric stretching of conjugated diene	Pentak, 2016
1580	−1	−1	−1	*N*-C═O	Stretching vibration carbonyl amide	Jain et al., 2016
1510	+2	+2	+1	C═C	Stretching of aromatic ring	Salaun & Vroman, 2009
1510	+1	+1	+1	C-NH	Asymmetric bending	Yadav, 2005
1491	−2	−2	−2	C═C	Aromatic ring stretching	Yadav, 2005
1448	−4	−4	−5	CH_2	C−H stretching vibration	Jain et al., 2016
1436	+1	−4	−3	C = CH_2	CH_2 deformation and bending	Sedeky et al., 2018
1350	−1	−1	−1	CH_2	Out of plane bending or twist, CH_2, wagging	Dutta & Bhattacharjee, 2017
1368	−2	−3	−2	C−H	Alkane C−H bond bending	Dutta & Bhattacharjee, 2017
1310	−2	−2	−2	C−N	C−N Asymmetric stretching	Silvertein, Webster, & Kiemle, 2005
1253	D	+1	+1	–O–CH_2–O–	C−O stretching from methylenedioxy	Saha, Seal, & Noor, 2013
1253	−2	−2	−2	C═C−O−C	Venyl ether stretching vibration	Saha et al., 2013
1194	0	0	0	C═C−O−C	Stretching vibration	Strunz, 2000
1133	D	D	D	–O–CH_2–O–	Ether group; methylene ether asymmetric stretching	Saha et al., 2013
1031	+2	+2	+1	C═C−O−C	Vinyl ether	Sedeky et al., 2018
1018	−1	−2	−1	C−H	Bending Trans CH = CH	Saha et al., 2013
996	−3	−3	−3	CH_2	Wagging vibrations	Strunz, 2000
930	−2	−2	−2	C−O	Methylendioxyphenyl	Field et al., 2008

0: not shifted; D: disappearance.
For least square regression analysis, a 0 value was assigned to not shifted or disappearance bands (D).
Negative value means an increase in frequency value, positive value means a decrease in frequency value shift NS:PIP = (pure piperine original frequency-piperine shifted frequency in the inclusion complex).

for 20 min using the Ultrasonic Processor model VC 505 (Sonics & Materials Inc., Kentucky, USA). The suspension was centrifuged at 2000 rpm for 10 min in the Neofuge 15R centrifuge (Heal Force, Shanghai, China). The supernatant was suitably diluted in ethanol and then analyzed in Synergy HT Multi-Modal Microplate Reader (Biotek, Vermont, USA) at 340 nm to determine the amount of PIP present in the NS. The LE was calculated using the following equation (Singireddy & Subramanian, 2014):

$$LE(\%) = \frac{Weight\ of\ PIP\ loaded\ in\ NS}{Initial\ weight\ of\ PIP\ fed\ for\ loading} x100 \quad (2)$$

2.6. Hyperspectral FTIR images

All NS samples loaded with PIP were prepared as pellets using a 7 mm KBr Pellet Quick Press with a die. The hyperspectral images of the pellets were obtained with a Perkin Elmer spotlight 400 FTIR system with a linear array detector (mercury cadmium telluride) and using an ATR cell equipped with a germanium crystal. Spectra were acquired using the Spectrum Image Spotlight 400 software (version 3.6.2) under the following conditions: spectral range of 4000–754 cm^{-1}, spectral resolution of 8 cm^{-1}, 16 scans per pixel, pixel size 6.25 × 6.25 μm and image size of 300 × 300 μm.

2.7. X-ray powder diffraction (XRPD)

NS samples were characterized using Multifunctional Smartlab diffractometer (Rigaku Corporation, Japan) with a Bragg-Brentano Theta-Theta goniometer. XRPD patterns were collected with k-alpha Cu radiation at 30 kV and 40 mA, with Ni filter, in the 3-60° 2θ range, counting 0.5°/s per step of 0.01°. Optical configuration of equipment employed a Rigaku D/teX 250 detector, 0.5° divergence slit, 5 mm antiscatter slit, and 5° Soller slits. Optical alignment was regularly checked against the NIST SRM660c LaB6 powder standard (Garrido et al., 2019).

2.8. Specific surface area

Specific surface area and pore structure properties of the NS samples were evaluated using NOVA 1000e (Quantachrome Instruments, Boyton Beach, Florida, USA). The degassing of the samples (1.0 g of the NS) was carried out at 120 °C for 24 h. The BET surface area was calculated from the adsorption isotherm using the multipoint BET method (Wilson, Mohamed & Headley, 2011).

2.9. Thermal analysis

Thermal properties of β-CD, NS, and NS:PIP (20.0 ± 0.001 g) were determined using a thermal analyzer (STA 6000, Perkin Elmer, San Diego, USA) that combines a thermogravimetric analyzer (TGA) with a differential scanning calorimeter (DSC). Nitrogen was used as purge and carrier gas at 70 and 40 mL/min, respectively. Samples were contained in ceramic pans. TGA analysis were conducted from 20 to 500 °C at a heating rate of 15 °C/min. β-CD, PIP, and a physical mixture (PM) of PIP with NS (PM-PIP-NS) were scanned as controls (Acevedo et al., 2018).

2.10. Statistical analysis

Three determinations were made for all assays and results were expressed as mean ± standard deviation. The analysis of variance and means comparison by Duncan's test were performed to determine significant differences at $p \leq 0.05$.

3. Results

3.1. NS synthesis

Initial screening was done to evaluate the effect of synthesis temperature (90, 120, 150 or 180 °C) on DS. It was found that high temperature tended to give high DS. Thus, for NS 1:6 and 1:10 M ratios of β-CD:DPC, 180 °C was used as the synthesis temperature. However, due to a high carbonization observed at 180 °C for NS with 1:2 M ratio of β-CD:DPC, 150 °C was used for the sample prepared with this

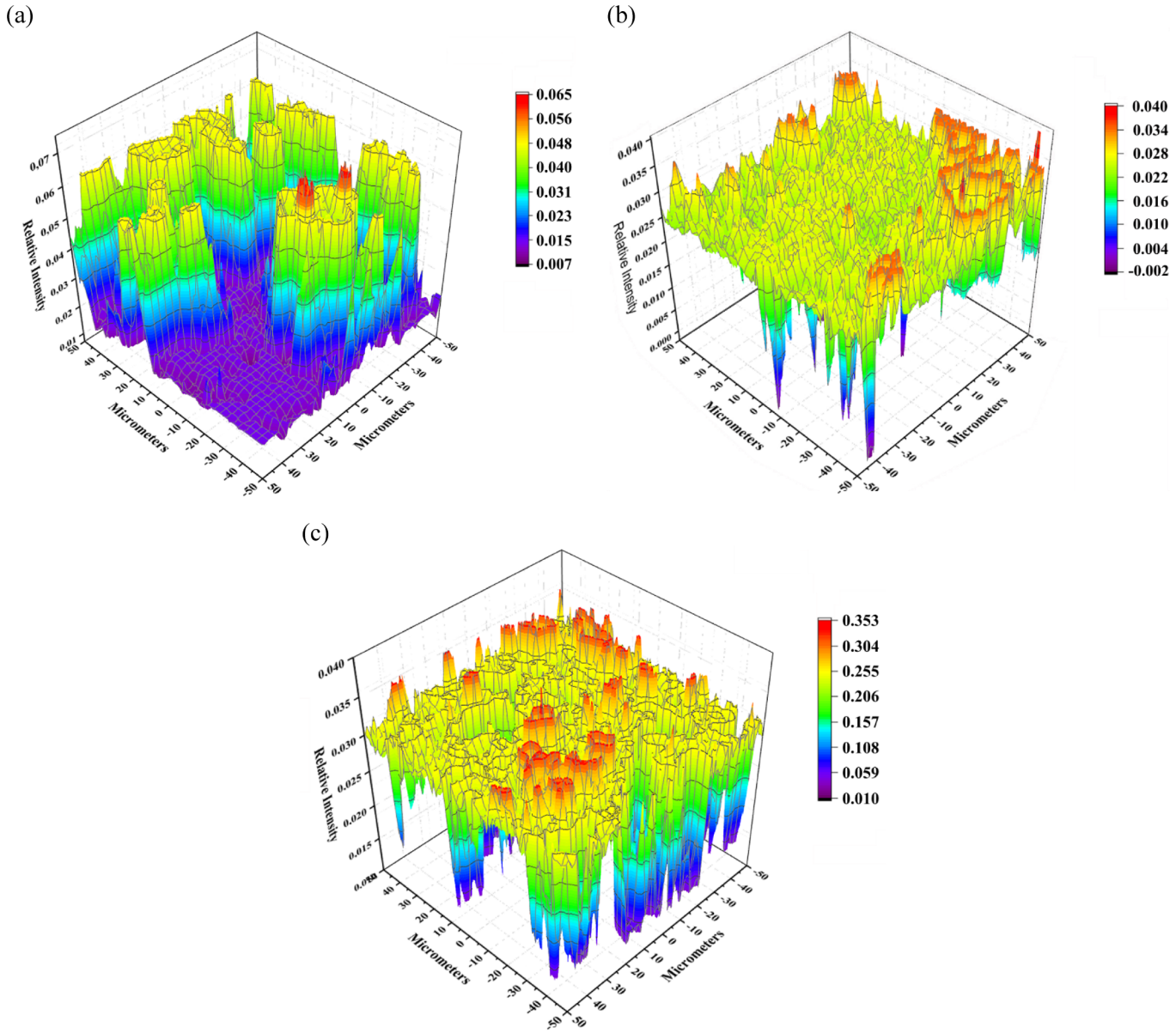

Fig. 3. Hyperspectral FTIR 3D images of piperine loaded in nanosponges at 1:2 (a), 1:6 (b) and 1:10 (c) β-cyclodextrin:diphenyl carbonate molar ratios at 1510 cm^{-1} due to stretching of aromatic ring associated with the formation of the nanosponge:piperine inclusion complex. (The figure must be in color).

formulation.

For all synthesis conditions tested, the formation of NS was confirmed by the FTIR analysis, due to the interaction of the hydroxyl groups of β-CD oriented outwards with the carbonate group of DPC (Caldera, Tannous, Cavalli, Zanetti & Trotta, 2017). The presence of the β-CD and NS characteristic peaks verified the stability of the β-CD structure after the NS synthesis (Garrido et al., 2019; Singireddy et al., 2016), as revealed by the appearance of the carbonyl group (1748 cm^{-1}) and the ester group (1256 cm^{-1}) in the IR spectra (Table 1). These bands suggested the crosslinking of β-CD through esterification reaction (Garrido et al., 2019). Also, by comparing the IR spectra of NS with that of the β-CD toroid, the presence of glycosidic bonds (C—O—C) and the β-CD ring breathing (at 945 cm^{-1}) revealed that the structure of the β-CD toroid was intact.

High DS values were observed for samples prepared with 30 min synthesis time at 1:2 and 1:6 β-CD:DPC molar ratios, as well as samples prepared with 15 min synthesis time at 1:10 β-CD:DPC molar ratio (Table 1). NS with high DS would have a greater number of crosslinks between the β-CD monomers (Osmani et al., 2018).

The DS was used for the selection of NS synthesis time, selecting the synthesis times with the highest DS for each of the β-CD: DPC molar ratios. These times were used to perform the corresponding NS characterization and bioactive charge analyses.

The XRPD spectra of NS samples (Fig. 1) were similar to that of β-CD, suggesting that the NS are crystalline structures. On the other hand, as the amount of DPC was increased in the NS synthesis, there was an increase in the intensity of counts per second (cps) of the narrow peaks. This observation indicated that NS crystallinity tended to increase with increasing crosslinking.

The S_{BET} values of NS with 1:2, 1:6 and 1:10 β-CD:DPC molar ratios, were 0.767, 1.224 and 1.967 $m^2\ g^{-1}$ respectively. An increase in S_{BET} was observed when the amount of crosslinking agent in the formulations was increased. This observation can be attributable to the presence of a greater amount of substituent involved in the synthesis reaction, resulting in the formation of increased crosslinking in the NS. As suggested by Caldera et al. (2017), the maximum value of the specific surface area that can be obtained in NS, based on crosslinking using carbonate, is 2 $m^2\ g^{-1}$, which is in the same order of magnitude to the

values obtained for NS prepared with 1:10 β-CD:DPC molar ratio in the present study.

The thermal analysis of NS by TGA showed peaks between 85 and 87 °C with mass losses of around 12%, attributable to the dehydration of the samples. High mass loss (73–74%) occurred around 324 °C due to the carbonization process of the samples (Data not shown). DSC thermograms (Fig. 2a) revealed one peak around 91–96 °C, and the second peak with higher intensity around 317 °C. The presence of the first peak is associated with the presence of moisture in the crystalline structure of the NS (Singireddy et al., 2016).

3.2. Piperine-loaded NS.

Both the NS type and the NS:PIP loading ratios had a significant effect ($p < 0.05$) on LE, whereas the solvent variable had no significant effect ($p > 0.05$) (Table 2). The LE of NS 1:10 β-CD:DPC was significantly higher ($p < 0.05$) than that of NS 1:2 β-CD:DPC, whereas the LE of NS 1:6 β-CD:DPC was not significantly different ($p > 0.05$) from those of 1:2 and 1:10 β-CD:DPC. This mean that a low amount of crosslinker can negatively affects the LE. According to Swaminathan et al. (2010), lower amount of crosslinker provide a low crosslinking of β-CD with decreased sites for bioactive complexation. Accordingly, the highest LE observed for NS 1:10 β-CD:DPC could be attributable to its large specific surface area derived from extensive β-CD network formation, which allowed an increase in PIP loading. On the other hand, the LE of NS was significantly lower ($p < 0.05$) at the 1:1 NS:PIP ratio than NS:PIP 1:2 and 2:1, for samples loaded using acetone and dichloromethane, but no significant differences were found in NS loaded using ethanol. Similarly, LE of NS was significantly lower at 1:1 NS:PIP ratio for NS 1:6 and 1:10 β-CD:DPC molar ratios, but no significant differences were found in the NS 1:2 β-CD:DPC molar ratio. The fact that in some conditions the LE of samples of 1:1 NS:PIP was lower than that of 1:2 and 2:1 NS:PIP was not expected and more research is needed to understand this better.

The formation of the NS:PIP inclusion complexes is evidenced by the shifts in the band frequency for PIP and NS FTIR spectra (Table 3). The characteristic vibration peaks of PIP in NS:PIP complexes were 930 cm^{-1} (methylenedioxyphenyl), 1031 cm^{-1} (vinyl ether), 1510 cm^{-1} (aromatic ring), 1580 cm^{-1} (carbonyl amide) and 1633 cm^{-1} (conjugated diene) (Field, Sternhell & Kalman, 2008; Jain, Meka & Chatterjee, 2016; Pentak, 2016; Salaun & Vroman, 2009; Sedeky, Khalil, Hefnawy & El-Sherbiny, 2018). The different NS used (12:2, 1:6 and 1:10 β-CD:DPC) in the formation of complexes with PIP have a similar behavior in terms of the displacements of their bands. Frequency shifts were observed in most of these bands associated with PIP, indicating the formation of inclusion complexes.

The DSC thermograms (Fig. 2b) of the inclusion complexes showed an endothermic peak. There was an increase in the enthalpy differences between the inclusion complexes and the physical mixture of PIP for NS derived from the three β-CD:DPC molar ratios. This observation again demonstrated the formation of inclusion complexes of PIP in the NS samples.

Fig. 3 shows the hyperspectral FTIR 3D images of PIP-loaded NS pellets, at 1510 cm^{-1} stretch aromatic ring of the PIP (Ezawa, Inoue, Murata, Takao, Sugita & Kanamoto, 2018; Quilaqueo et al., 2019), allowing one to identify the PIP distribution in NS. Areas with red color (higher intensity) indicate the presence of high concentration of PIP, while areas with dark blue (lower intensity) indicate low PIP concentration. As shown, PIP was distributed in a dispersed manner for the NS:PIP complex at 1:2 β-CD:DPC molar ratio, while NS:PIP complexes at 1:6 and 1:10 β-CD:DPC molar ratios showed relatively more homogenous PIP distribution. This observation is consistent with the higher S_{BET} and LE values for NS:PIP 1:1, where higher PIP loadings were observed due to increased crosslinking between the β-CD monomers.

4. Conclusion

This study demonstrated the feasibility of using microwave-assisted fusion to synthesize NS with a high DS to be loaded with PIP. In NS samples with 1:6 and 1:10 β-CD:DPC molar ratios, there was an increase in DS, S_{BET} and crystallinity, resulting in NS with a greater surface area. Similarly, NS with a higher degree of crosslinking had a high LE of PIP. As NS can encapsulate PIP with a high LE, they could be used in pharmaceutical or food formulations. However, analysis of the release kinetics of PIP under gastrointestinal conditions should be performed in order to establish how the variable degree of cross-linking affects the release kinetics of PIP.

Credit authorship contribution statement

Juan Guineo-Alvarado: Conceptualization, Methodology, Formal analysis, Investigation, Writing - original draft. **Marcela Quilaqueo:** Writing - review & editing. **Jeyson Hermosilla:** Formal analysis. **Sofía González:** Methodology, Formal analysis. **Camila Medina:** Investigation. **Aldo Rolleri:** Resources. **Loong-Tak Lim:** Writing - review & editing. **Mónica Rubilar:** Project administration.

Declaration of Competing Interest

The authors declare that they have no known competing financial interests or personal relationships that could have appeared to influence the work reported in this paper.

Acknowledgements

This research was funded by CONICYT through FONDECYT project N° 1160558 and by Research office from Universidad de La Frontera. We are also grateful to projects FONDEQUIP EQM150019 and FONDEQUIP EQM160152 for granting access to their equipment and to Dr. Helen Lowry for her support in editing the English in the manuscript.

References

Acevedo, F., Hermosilla, J., Sanhueza, C., Mora-Lagos, B., Fuentes, I., Rubilar, M., Concheiro, A., & Alvarez-Lorenzo, C. (2018). Gallic acid loaded PEO-core/zein-shell nanofibers for chemopreventive action on gallbladder cancer cells. *European Journal of Pharmaceutical Sciences, 119*, 49–61. https://doi.org/10.1016/j.ejps.2018.04.009.

Astray, G., Gonzalez-Barreiro, C., Mejuto, J. C., Rial-Otero, R., & Simal-Gándara, J. (2009). A review on the use of cyclodextrins in foods. *Food Hydrocolloids, 23*(7), 1631–1640.

Astray, G., Mejuto, J. C., Morales, J., Rial-Otero, R., & Simal-Gándara, J. (2010). Factors controlling flavors binding constants to cyclodextrins and their application in foods. *Food Research International, 43*, 1212–1218.

Bardts, M., Gonsior, N., & Ritter, H. (2008). Polymer Synthesis and Modification by Use of Microwaves. *Macromolecular Chemistry and Physics, 209*(1), 25–31. https://doi.org/10.1002/macp.200700443.

Bogdal, D., Penczek, P., Pielichowski, J., & Prociak, A. (2003). Microwave assisted synthesis, crosslinking, and processing of polymeric materials. *Advances in Polymer Science, 163*, 193–263. https://doi.org/10.1007/b11051.

Caldera, F., Tannous, M., Cavalli, R., Zanetti, M., & Trotta, F. (2017). Evolution of Cyclodextrin Nanosponges. *International Journal of Pharmaceutics, 531*(2), 470–479. https://doi.org/10.1016/j.ijpharm.2017.06.072.

Challa, R., Ahuja, A., Ali, J., & Khar, R. K. (2005). Cyclodextrins in drug delivery: An updated review. *AAPS PharmSciTech, 6*(2), E329–E357. https://doi.org/10.1208/pt060243.

Cid, A., Astray, G., Morales, J., Mejuto, J. C., & Simal-Gandara, J. (2018). Influence of β-cyclodextrins upon the degradation of carbofuran derivatives under alkaline conditions. *Journal of Pesticides and Biofertilizers, 1*, 1–4.

Dutta, S., & Bhattacharjee, P. (2017). Nanoliposomal encapsulates of piperine-rich black pepper extract obtained by enzyme-assisted supercritical carbon dioxide extraction. *Journal of Food Process Engineering, 201*, 49–56. https://doi.org/10.1016/j.jfoodeng.2017.01.006.

Ezawa, T., Inoue, Y., Murata, I., Takao, K., Sugita, Y., & Kanamoto, I. (2018). Characterization of the dissolution behavior of piperine/cyclodextrins inclusion complexes. *International Journal of Medicinal Chemistry, 19*, 923–933. https://doi.org/10.1155/2016/8723139.

Field, L.D., Sternhell, S., & Kalman, J.R. (2008). Organic Structures from Spectra. (4th Ed.

). Sydney: John Wiley & Sons.
Gaidamauskas, E., Norkus, E., Butkus, E., Crans, D. C., & Grincienė, G. (2009). Deprotonation of β-cyclodextrin in alkaline solutions. *Carbohydrate Research, 344*(2), 250–254. https://doi.org/10.1016/j.carres.2008.10.025.
Garrido, B., González, S., Hermosilla, J., Millao, S., Quilaqueo, M., Guineo, J., Acevedo, F., Pesenti, H., Rolleri, A., Shene, C., & Rubilar, M. (2019). Carbonate-β-Cyclodextrin-Based Nanosponge as a Nanoencapsulation System for Piperine: Physicochemical Characterization. *Journal of Soil Science and Plant Nutrition, 19*(3), 620–630.
Hoogenboom, R., & Schubert, U. S. (2007). Microwave-assisted polymer synthesis: Recent developments in a rapidly expanding field of reserch. *Macromolecular Rapid Communications, 28*, 368–386. https://doi.org/10.1002/marc.200600749.
Jain, S., Meka, S. R. K., & Chatterjee, K. (2016). Engineering a Piperine Eluting Nanofibrous Patch for Cancer Treatment. *ACS Biomaterials Science & Engineering, 2*(8), 1376–1385. https://doi.org/10.1021/acsbiomaterials.6b00297.
Minelli, R., Cavalli, R., Ellis, L., Pettazzoni, P., Trotta, F., Ciamporcero, E., Barrera, G., Fantozzi, R., Dianzani, C., & Pili, R. (2012). Nanosponge-encapsulated camptothecin exerts anti-tumor activity in human prostate cancer cells. *European Journal of Pharmaceutical Sciences, 47*(4), 686–694. https://doi.org/10.1016/j.ejps.2012.08.003.
Osmani, R.A.M., Kulkami, P.K., Gowda, V., Hani, U., Gupta, V.K., Prerana, M., & Saha, C. (2018). Cyclodextrin based nanosponges in drug delivery and cancer therapeutics: new perspectives for old problems. In: D. Inamuddin,A. Asiri, & A. Mohammad (Eds.), Applications of nanocomposite materials in drug delivery (pp. 97-147). Mysuru:Woodhead Publishing.
Pentak, D. (2016). In vitro spectroscopic study of piperine-encapsulated nanosize liposomes. *European Biophysics Journal, 45*(2), 175–186. https://doi.org/10.1007/s00249-015-1086-x.
Pushpalatha, R., Selvamuthukumar, S., & Kilimozhi, D. (2018). Cross-linked, cyclodextrin-based nanosponges for curcumin delivery - Physicochemical characterization, drug release, stability and cytotoxicity. *Journal of Drug Delivery Science and Technology, 45*, 45–53. https://doi.org/10.1016/j.jddst.2018.03.004.
Quilaqueo, M., Millao, S., Luzardo-Ocampo, I., Campos-Vega, R., Acevedo, F., Shene, C., & Rubilar, M. (2019). Inclusion of piperine in β-cyclodextrin complexes improves their bioaccessibility and in vitro antioxidant capacity. *Food Hydrocolloids, 91*, 143–152. https://doi.org/10.1016/j.foodhyd.2019.01.011.
Rao, M., Bajaj, A., Khole, I., Munjapara, G., & Trotta, F. (2012). In vitro and in vivo evaluation of β-cyclodextrin-based nanosponges of telmisartan. *Journal of Inclusion Phenomena and Macrocyclic Chemistry, 77*(1-4), 135–145. https://doi.org/10.1007/s10847-012-0224-7.
Rao, M. R. P., & Bhingole, R. C. (2015). Nanosponge-based pediatric-controlled release dry suspension of Gabapentin for reconstitution. *Drug Development and Industrial Pharmacy, 41*(12), 2029–2036. https://doi.org/10.3109/03639045.2015.1044903.
Rakmai, J., Cheirsilp, B., Mejuto, J. C., Simal-Gándara, J., & Torrado-Agrasar, A. (2018). Antioxidant and antimicrobial properties of encapsulated guava leaf oil in hydroxypropyl-beta-cyclodextrin. *Industrial Crops and Products, 111*, 219–225.
Rakmai, J., Cheirsilp, B., Mejuto, J. C., Torrado-Agrasar, A., & Simal-Gándara, J. (2017). Physico-chemical characterization and evaluation of bio-efficacies of black pepper essential oil encapsulated in hydroxypropyl-beta-cyclodextrin. *Food Hydrocolloids, 65*, 157–164.
Rakmai, J., Cheirsilp, B., Torrado-Agrasar, A., Simal-Gándara, J., & Mejuto, J. C. (2017). Encapsulation of yarrow essential oil in hydroxypropyl-beta-cyclodextrin: Physicochemical characterization and evaluation of bio-efficacies. *CYTA-Journal of Food, 2017*, 1–9.
Saha, K. C., Seal, H. P., & Noor, M. A. (2013). Isolation and characterization of piperine from the fruits of black pepper (Piper nigrum). *Journal of Bangladesh Agricultural University, 11*, 11–16. https://doi.org/10.3329/jbau.v11i1.18197.
Salaun, F., & Vroman, I. (2009). Curcumin-loaded nanocapsules: Formulation and influence of the nanoencapsulation processes variables on the physico-chemical characteristics of the particles. *International Journal of Chemical Reactor Engineering, 7*, 1–26. https://doi.org/10.2202/1542-6580.2093.
Sedeky, A. S., Khalil, I. A., Hefnawy, A., & El-Sherbiny, I. M. (2018). Development of core-shell nanocarrier system for augmenting piperine cytotoxic activity against human brain cancer cell line. *European Journal of Pharmaceutical Sciences, 118*, 103–112. https://doi.org/10.1016/j.ejps.2018.03.030.
Shityakov, S., Bigdelian, E., Hussein, A. A., Hussain, M. B., Tripathi, Y. C., Khan, M. U., & Shariati, M. A. (2019). Phytochemical and pharmacological attributes of piperine: A bioactive ingredient of black pepper. *European Journal of Medicinal Chemistry, 176*, 149–161. https://doi.org/10.1016/j.ejmech.2019.04.002.
Shringirishi, M., Prajapati, S. K., Mahor, A., Alok, S., Yadav, P., & Verma, A. (2014). Nanosponges: A potential nanocarrier for novel drug delivery-a review. *Asian Pacific Journal of Tropical Disease, 4*, S519–S526. https://doi.org/10.1016/S2222-1808(14)60667-8.
Silvertein, R. M., Webster, F. X., & Kiemle, D. J. (2005). *Spectrometric identification of organic compounds* (7th ed.). New York: John Wiley & Sons, INC.
Singireddy, A., Pedireddi, S. R., Nimmagadda, S., & Subramanian, S. (2016). Benefical effects of microwave assisted heating versus conventional heating in synthesis of ciclodextrin based naosponges. *Materials Today: Proceedings, 3*, 3951–3959. https://doi.org/10.1016/j.matpr.2016.11.055.
Singireddy, S., & Subramanian, S. (2014). Fabrication of cyclodextrin nanosponges for quercetin delivery: Physicochemical characterization, photostability, and antioxidant effects. *Journal of Materials Science, 49*(23), 8140–8153. https://doi.org/10.1007/s10853-014-8523-6.
Subramanian, S., Singireddy, A., Krishnamoorthy, K., & Rajappan, M. (2012). Nanosponges: a novel class of drug delivery system–review. Journal of Pharmacy & Pharmaceutical Sciences, 15, 103-111. https://doi.org/10.18433/J3K308.
Swaminathan, S., Pastero, L., Serpe, L., Trotta, F., Vavia, P., Aquilano, D., Trotta, M., Zara, GianPaolo, & Cavalli, R. (2010). Cyclodextrin-based nanosponges encapsulating camptothecin: Physicochemical characterization, stability and cytotoxicity. *European Journal of Pharmaceutics and Biopharmaceutics, 74*(2), 193–201. https://doi.org/10.1016/j.ejpb.2009.11.003.
Swapna, P. R. D., Junise, V., Shibin, P., Senthila, S., & Rajesh, R. S. (2012). Isolation, identification and antimycobacterial evaluation of piperine from Piper longum. *Der Pharmacia Letter, 4*, 863–868.
Tejashri, G., Amrita, B., Darshana, J. (2013). Cyclodextrin based nanosponges for pharmaceutical use: a review. Acta Pharmaceutica, 63, 335–358. https://doi.org/10.2478/acph-2013-0021.
Trotta, F., Moraglio, G., Marzona, M., & Maritano, S. (1993). Acyclic carbonates of β-cyclodextrin. *Gazzetta Chimica Italiana, 123*, 559–562.
Wiesbrock, F., Hoogenboom, R., & Schubert, U. S. (2004). Microwave-Assisted Polymer Synthesis: State-of-the-Art and Future Perspectives. *Macromolecular Rapid Communications, 25*(20), 1739–1764. https://doi.org/10.1002/marc.200400313.
Wilson, L. D., Mohamed, M. H., & Headley, J. V. (2011). Surface area and pore structure properties of urethane-based copolymers containing β-cyclodextrin. *Journal of Colloid and Interface Science, 357*(1), 215–222. https://doi.org/10.1016/j.jcis.2011.01.081.
Yadav, L. D. S. (2005). *Organic Spectroscopy*. Bangladesh: Springer-Science Bussiness Media, B.V.
Zarai, Z., Boujelbene, E., Ben Salem, N., Gargouri, Y., & Sayari, A. (2013). Antioxidant and antimicrobial activities of various solvent extracts, piperine and piperic acid from Piper nigrum. *LWT - Food Science and Technology, 50*(2), 634–641. https://doi.org/10.1016/j.lwt.2012.07.036.